HTS Step-edge Josephson Junction Terahertz Harmonic Mixer

Jia Du[1], Andrew R. Weily[2], Xiang Gao[1], Ting Zhang[2], Cathy P. Foley[1], Yingjie Jay Guo[3]

[1] CSIRO Manufacturing, PO Box 218, Lindfield, NSW 2070, Australia;

[2] CSIRO Data 61, Marsfield, NSW 1710, Australia;

[3] Global Big Data Technologies Centre, University of Technology, Sydney, Ultimo, NSW 2007, Australia

Abstract

A high-temperature superconducting (HTS) terahertz (THz) frequency down-converter or mixer based on a thin-film ring-slot antenna coupled $YBa_2Cu_3O_{7-x}$ (YBCO)/MgO step-edge Josephson junction is reported. The frequency down-conversion was achieved using higher order harmonics of an applied lower frequency (19-40 GHz) local oscillator signal in the Josephson junction mixing with a THz signal of over 600 GHz, producing a 1-3 GHz intermediate frequency signal. Up to 31st order of harmonic mixing was obtained and the mixer operated stably at temperatures up to 77 K. The design details of the antenna, HTS Josephson mixer, the matching and isolation circuits, and the DC and RF performance evaluation are described in this paper.

Introduction

The unprecedented growth in the development of wireless communication systems has pushed operating frequencies towards the millimetre and lower terahertz (THz) frequency range. The large amount of bandwidth available at THz frequencies will enable fast transmission of huge amounts of data as needed for new emerging applications. Research on THz communications has received increased attention in recent years [1]. New developments to improve the performance of sources and detectors, circuits, antenna technology, and system architecture are required to realize ultrafast THz data transmission. Due to extensive transmission loss in the atmosphere of millimetre and THz waves, ultrahigh-sensitive heterodyne receiver front-ends or mixers are needed to compensate for the propagation loss.

High-temperature superconducting (HTS) Josephson junctions are promising candidates for THz band detectors and mixers due to their special properties, such as low noise, low power consumption, broadband and high frequency operation (well into THz band) as a result of the high-energy band gap. Compared to the low-temperature superconducting (LTS) devices, HTS devices offer an obvious practical advantage of operating at higher temperatures so that cheaper and simpler cryogenic instruments (for example, miniature size portable cryocoolers) can be used. HTS THz direct detectors based on bicrystal [2, 3] and step-edge [4, 5] grain-boundary junctions have been developed in recent years. These HTS detectors are, however, not suitable for use in communication systems as they only measure the amplitude of THz signal power not the phase information that is required for telecommunication applications. Recently, HTS Josephson heterodyne frequency down-converters or mixers based on CSIRO step-edge junction technology were demonstrated in the microwave frequency range up to 30 GHz [6, 7].

There have been very limited reports of successful demonstration of HTS Josephson junction THz mixers [8 -10] due to the challenges of producing reliable and high quality HTS Josephson junctions and inaccessible instruments and components at THz frequency bands. The reported HTS THz mixers in the literature mostly operate at temperatures significantly lower than 77K (for example, 10 and 20K [8, 9] and 50K [10]) and at frequencies lower than reported in this paper. For heterodyne mixing in the submillimeter and THz wave regions, it is difficult to obtain a tunable high frequency local oscillator (LO) for fundamental mixing. Consequently, Josephson junction harmonic mixing would be a particularly useful technique. Josephson junction harmonic mixers have been mostly observed in LTS SIS (superconductor-insulator-superconductor) junctions at microwave and millimeter frequencies [11, 12]. Chen et al [13] observed high order harmonic mixing well into THz frequency range in HTS bicrystal junctions, but no details of mixer performance were given. Harmonic mixing

In this paper, we report our first demonstration of a HTS step-edge junction THz heterodyne mixer using high-order harmonic mixing. The advantage of such a harmonic mixer is to remove the need of using a second expensive THz signal source as the LO pumping source thus simplifying the system architecture and reducing the system cost and size. A thin-film antenna and microwave matching circuit were designed to couple the THz signal and LO signal into the Josephson junction mixer and extract the down-converted IF signal.

Design of Antenna, Matching and Isolation Circuits for the Josephson Harmonic Mixer

The schematic layout of the antenna-coupled HTS Josephson junction mixer and matching circuit is shown in Figure 1. The aims of the mixer and bias-tee design are to create a low-loss path from the

Josephson junction mixer to the LO and IF ports, while maintaining high isolation between the RF, LO, IF and DC ports. The mixer is fabricated on a 0.5 mm thick MgO substrate (ε_r = 9.65, tanδ = 0.0005), which then couples to a 3 mm diameter high resistivity silicon hemispherical lens (ε_r = 11.9, tanδ = 0.00025). The step-edge Josephson junction is placed across the circular slot of a thin-film ring-slot antenna as shown in the enlarged inset in Figure 1. The ring-slot antenna has a truncated circular ground plane and a coplanar waveguide (CPW) feed network that attaches to a CPW low-pass filter (LPF) with a -3dB cut-off frequency of approximately 250 GHz. This ring-slot/CPW combination is similar to that used previously for amplitude detection [4], but has been adapted here for use as a harmonic mixer and its parameters optimized to give peak realized gain around 620 to 640 GHz. The LPF is connected to a tapered CPW line for efficient coupling to the bias-tee circuit, such that the width of the CPW centre conductor matches the width of the microstrip line with a characteristic impedance of 50 Ω. The tapered CPW line also acts as a LPF, with a -3dB cut-off frequency of approximately 100GHz, and serves to filter the THz signal received by the ring-slot antenna from the LO and IF ports.

The bias-tee was designed to provide isolation between the DC bias current applied to the HTS junction and the LO and IF signals of the mixer circuit, and to be wideband to enable flexibility in the choice of the LO frequency that drives the mixer. It was implemented on a 254 μm thick polished Alumina substrate (ε_r = 9.9, tanδ = 0.0002) with a 3 μm TiW/Au metallization. Both the bias circuit and ring-slot antenna were designed using the software CST Microwave Studio. To the left of the bias-tee is a diplexer circuit, that consists of a high-pass filter (HPF) and a LPF to separate the LO and IF signals. This circuit is located external to the cryocooler, it has a LPF passband from DC to 17 GHz, a HPF passband from ~19 to 40 GHz, and a typical isolation of 50 dB.

In the mixer prototype, two ring-slot antennas are included in a single 10mm × 10 mm substrate and the schematic of the mixer prototype is shown in Figure 2. A single hemispherical lens of 3mm diameter is placed on the back of the substrate. The centre-to-centre distance between the two ring-slot antennas is 300 μm, which makes the offset from the ring-slot to centre of the lens 150 μm. The port labels are used for analysis using CST Microwave Studio. Ports 1 and 3 correspond to the location of the Josephson junctions, and the normal resistance R_n of the junction has been estimated to be between 2 Ω and 4 Ω. Ports 2 and 4 correspond to the CPW transmission line ports, which connect to bias-tees as described in Figure 1. Computed realized gain of the lens/ring-slot antenna combination as a function of frequency for two different values of the junction resistance R_n is presented in Figure 3, where realized gain includes both ohmic and mismatch losses due to the low normal resistance of the junction, and Port 1 is excited. It can be seen that higher R_n value results in

better antenna gain due to better impedance matching. In this experiment, an R_n value of 4 Ω was measured. A peak realized gain of 18.2dBi is computed at 640 GHz, and the realized gain is greater than 15 dBi from 590 to 670 GHz. Radiation patterns for the E-plane have also been computed for the lens/ring-slot antenna and are depicted in Figure 4. There is a 15° beam squint in the E-plane due to the 150 um offset of the ring-slot antenna from the centre of the lens. Computed half power beamwidth (HPBW) is 11° in both the E-plane and H-plane at 620 GHz. To show the coupling efficiency, the S-parameters of the dual ring-slot feed have also been computed and are shown in Figure 5. Coupling (S_{21}) from the Josephson junction at P1 to P2 shows the loss in the LO and IF signal chains and is 5±1 dB from 0 to 30 GHz. Coupling from P1 to the ports of the adjacent ring-slot antenna (P3 and P4) is also important to show there is sufficient isolation between the two antennas. Figure 5 shows that the RF isolation (S_{31}) between the Josephson junction ports is greater than 25 dB at 620 GHz, and the LO/IF isolation (S_{41}) of Port 4 from the RF signal at Port 1 is better than 50 dB from 0 to 30 GHz. The computed reflection coefficient, S_{11}, at the ring-slot (P1) is -2.8 dB at 620 GHz; this value is low due to the relatively small normal resistance of the Josephson junction. Improvement to the matching can be achieved by further increasing the junction normal resistance, a subject of the on-going HTS junction parameter optimisation.

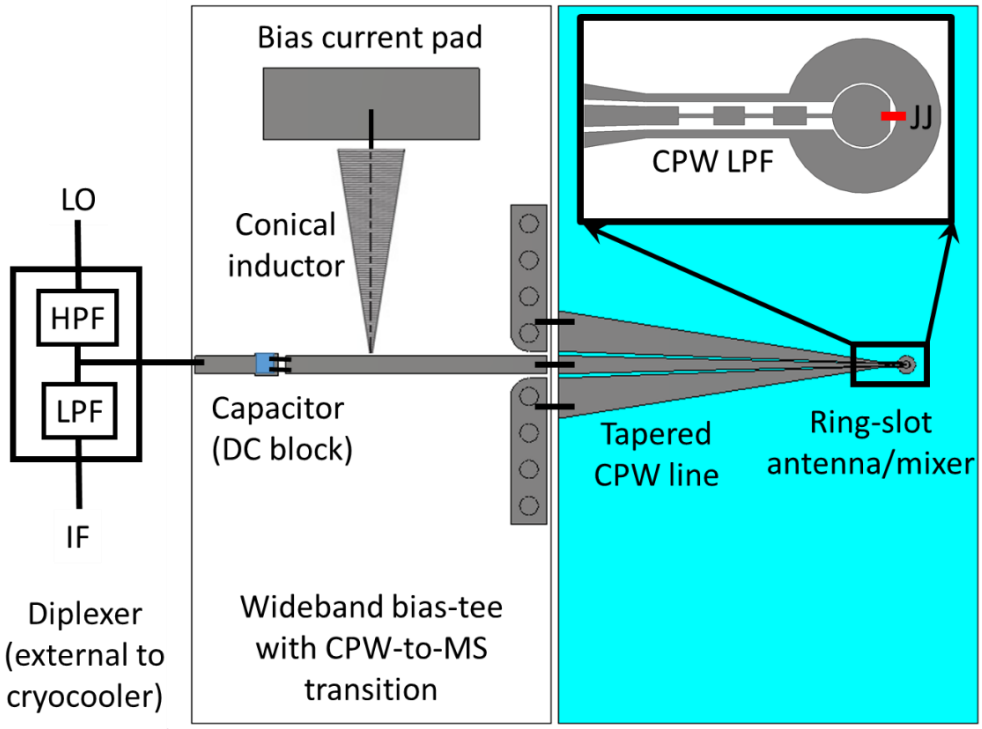

Figure 1. Schematic diagram of THz harmonic mixer. Inset shows an enlarged view of the THz ring-slot antenna and the location of the Josephson junction (JJ).

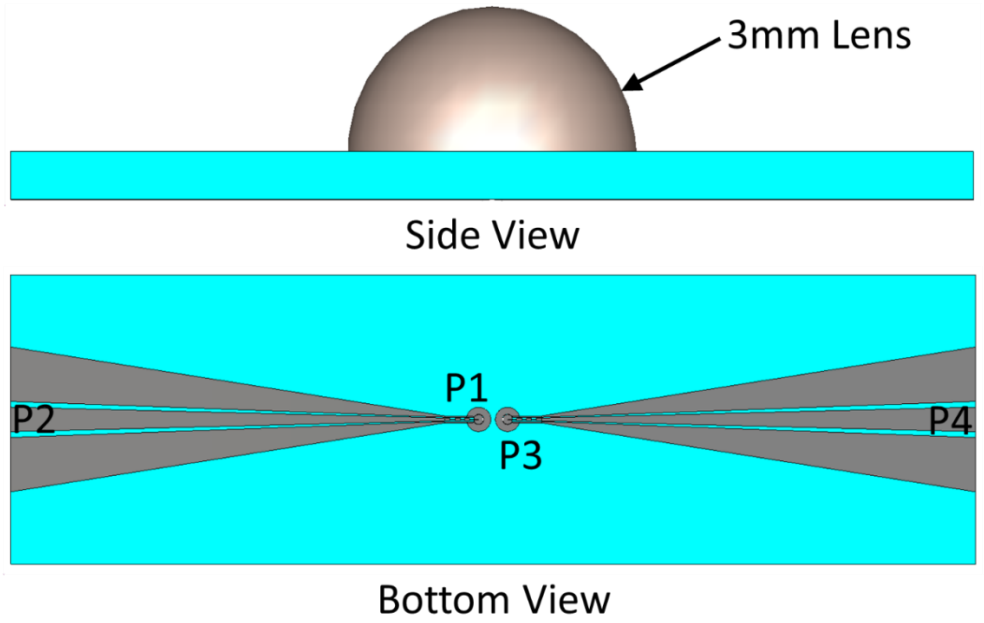

Figure 2. Side view and bottom view of two THz ring-slot antennas coupled to a single 3mm hemispherical lens, including port number labels.

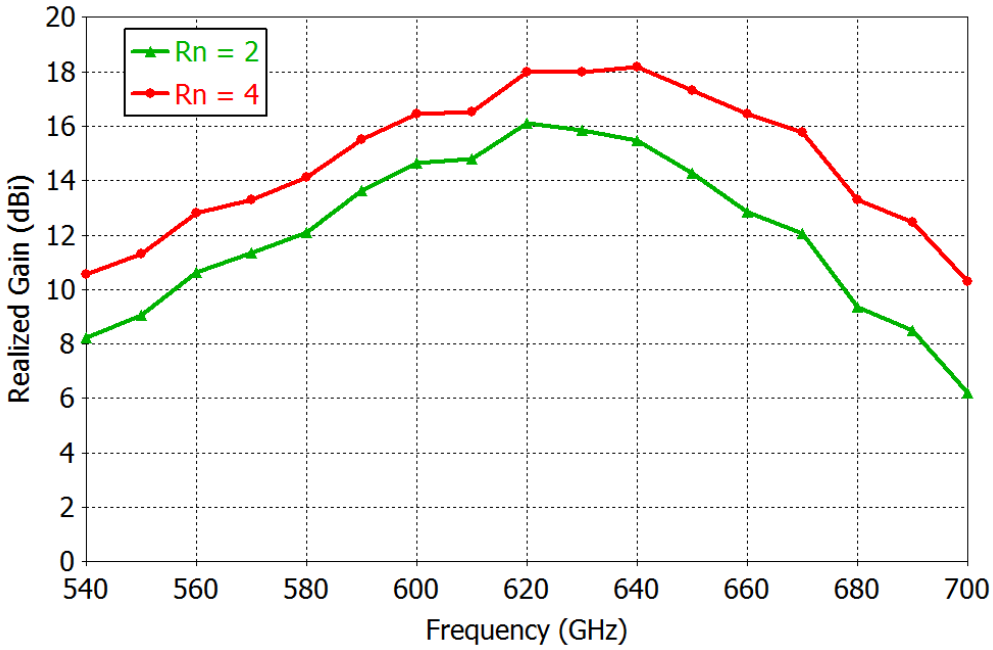

Figure 3. Computed realized gain of the THz ring-slot antenna with the lens for two difference R_n values of the HTS junction.

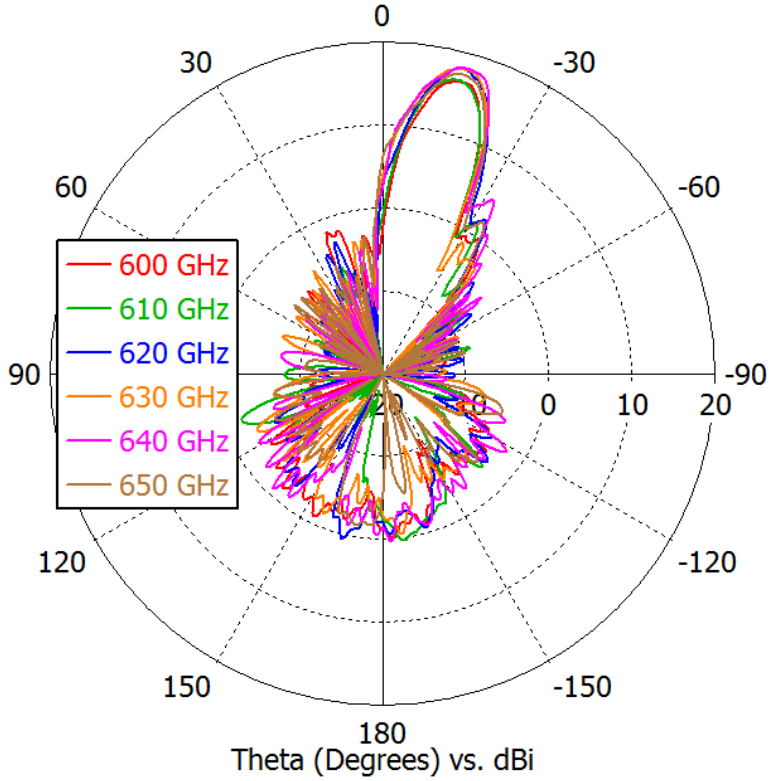

Figure 4. Computed E-plane radiation patterns of the THz ring-slot antenna from 600 to 650 GHz.

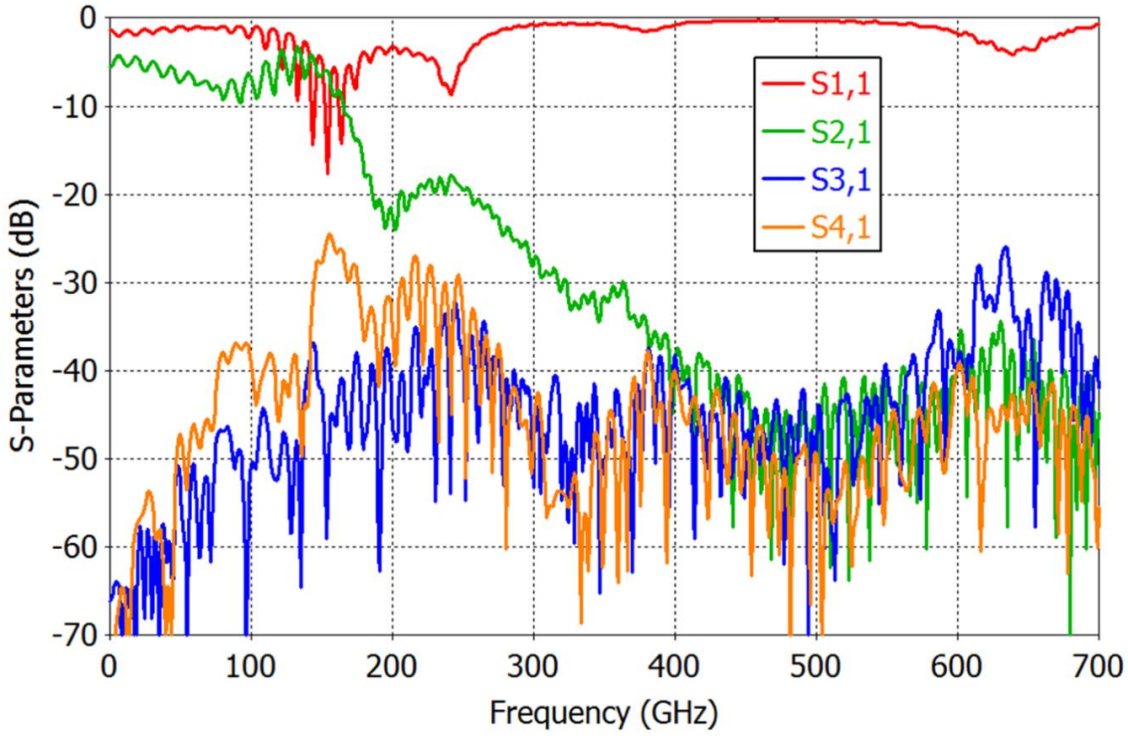

Figure 5. Computed S-parameters of two THz ring-slot antennas coupled to a single 3mm lens.

Experimental Details

The device was fabricated using the established step-edge $YBa_2Cu_3O_{7-x}$ (YBCO) junction technology developed at CSIRO [14, 15]. The 10 mm × 10 mm × 0.5 mm MgO substrate was first patterned and etched using a standard photolithography and Ar-ion beam etching techniques to create a step-edge pattern with ~ 400 nm height and ~ 35° angle. A 200 nm thick YBCO film with a 50 nm in-situ Au film on top was deposited on the processed MgO substrate by Ceraco GmbH. The YBCO film was then patterned and etched to form the step-edge junctions and the DC bias lines. The in-situ Au was removed from the junction area but remained on the DC lines and contact pads for achieving lower contact resistance and bondable pads [16]. Additional layer of ~ 300 nm Au thin film was deposited using dc sputtering technique and patterned to form the Au thin-film antenna.

Figure 6 shows the micrographs of the fabricated chip ((a) and (b)) and the photographs of the packaged mixer module ((c) and (d)). The ring slot antennas with the tapered CPW lines are made from the Au thin-film and the Josephson junctions are the 2 μm wide narrow YBCO micro strips across the step patterns located in the ring slots as shown in the enlarged view in (b). Two mixer devices were made on a single 10x10 mm MgO substrate with the in-house designed bias-tee on both sides to obtain two mixer modules in one package. The fabricated YBCO/MgO substrate with two PCB bias tee circuits were mounted into a specially designed Au-coated copper housing. The series inductors and shunt capacitors were mounted on the bias tee PCBs ((c)) which are used to block the DC signals from the LO and IF ports and to block the RF, LO and IF signals from the DC bias port. DC and RF wire connections were made using ultrasonic Au ribbon bonding. The top eight colored wires in Figure (c) are the DC bias lines connected via surface mount capacitors and resistors. As shown in Figure (d), a 3 mm diameter high resistivity silicon hyper-hemispherical lens was bonded to the reverse side of the substrate for coupling the THz signal. The combination of the MgO substrate and hemispherical silicon lens forms a lens which ensures a high antenna directivity and efficient coupling between free-space and the antennas.

The packaged THz HTS mixer was cooled on a commercial 2-stage pulse-tube cryocooler (PTC). In this experiment, the DC and RF mixing properties were characterized at operating temperatures from 40 to 77K, a temperature range that is potentially attainable with a single-stage mini cryocooler thus demonstrating the full potential of a HTS THz mixer for practical applications. A compact commercial solid-state THz source (VDI 625 GHz Amplifier Multiplier Chain) was used to generate THz radiation between 590 and 650 GHz. The THz signal, after passing through a pair of collimating and focusing mirrors, was focused onto the HTS mixer module via the Si lens through the cryocooler window. The LO pumping signal was supplied using an Agilent Technologies E8257D signal generator

for frequencies up to 20 GHz or an Anritsu 68087C signal generator for frequencies up to 40 GHz. For harmonic mixing, the LO and IF signals share the same port of the mixer module and the IF signal was isolated by using a microwave diplexer connected outside of the cryocooler. The mixer IF output was amplified using a room temperature low-noise-amplifier (LNA) and displayed on an Agilent E4407B spectrum analyzer. A battery-powered DC current source was used to bias the Josephson mixer.

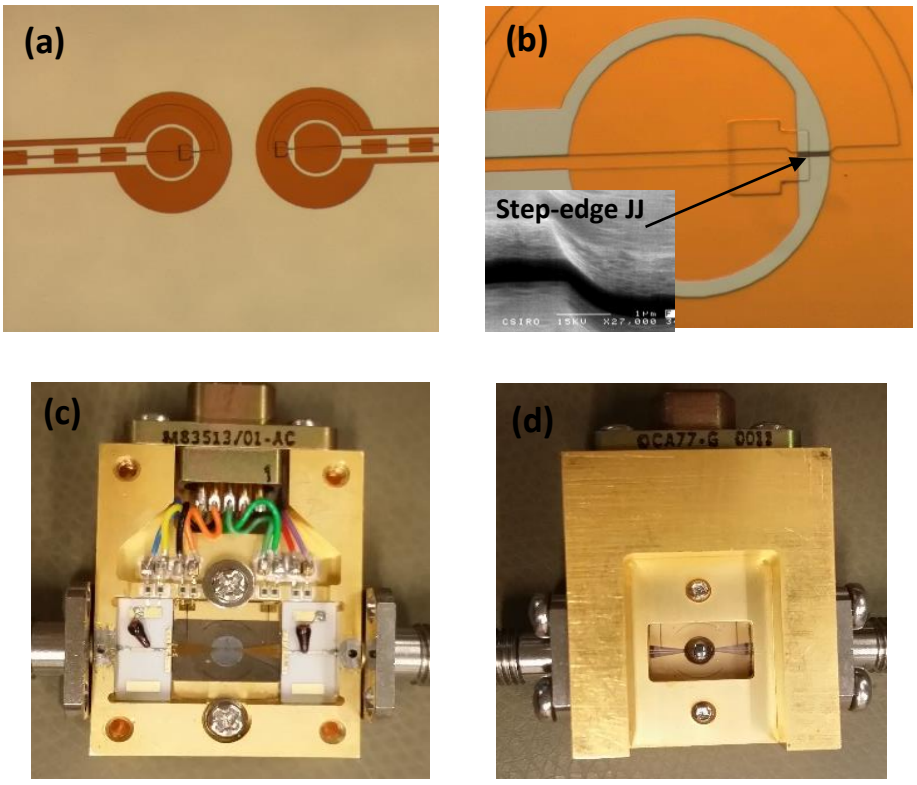

Figure 6 (a) and (b) are photographs of the fabricated device chip containing two antenna-coupled HTS Josephson mixers; (b) shows a 2 μm wide YBCO micro-strip line (black colour) across a step-edge on the MgO substrate inside the slot forming a step-edge junction which connects the inner and outer conductors of the antenna. The inset in (b) is a scanning electron micrograph (SEM) graph of the step-edge junction. (c) and (d) are photographs of the packaged module showing on the circuit side (c) and the backside (d) where a 3mm Si lens is attached onto the back of MgO substrate for coupling the THz signal onto the antenna and junction.

Results and Discussion

Figure 7 shows the DC current-voltage characteristics (IVCs) of the step-edge junction at different operating temperatures from 40K to 77K. The junction demonstrated a resistively-shunted-junction behaviour with a normal resistance $R_n \approx 4\ \Omega$. The junction critical current, I_c, increases with

decreasing temperature, from 25 μA at 77 K to 500 μA at 40 K. The junction characteristic voltage, $V_c \equiv I_cR_n$, versus the temperature is plotted in the inset of the figure. The I_cR_n value increases from 100 μV at 77 K to 2 mV at 40 K, which corresponds to a junction characteristic frequency, $f_c \equiv I_cR_n/\Phi_0$ (where Φ_0 is the magnetic flux quantum, $1/\Phi_0 \equiv 2e/h = 0.4836$ GHz/μV), of ~ 50 GHz at 77 K to ~ 1 THz at 40 K. The characteristic frequency value of the junction shows it is well suited as a THz frequency down-converter or mixer. By changing operating temperature, the junction parameters can be adjusted to enable RF detection and mixing across a very wide frequency range. This is an additional advantage of using a temperature-adjustable cryocooler instead of liquid nitrogen, though we can tune our fabrication process to optimise the junction characteristics for use at a given fixed temperature.

As shown in Figure 7, the dynamic resistance, $R_D = dV/dI$, increases with decreasing the temperature which should result in an increase of the mixer conversion efficiency (η) as shown by the equation below [17].

$$\eta = P_{IF}/P_{RF} = \frac{C_{IF}R_D}{8}\left(\frac{\partial(I_c)}{\partial(P_{LO})^{1/2}}\right)^2 \quad (1)$$

where C_{IF} is the output coupling efficiency (≤ 1), P_{LO} is the available power from the LO source, I_c is the junction critical current under the operating conditions (suppressed by P_{LO}). Eq. (1) shows the conversion efficiency scales with R_D and the differential dependence of I_c on P_{LO}. In this experiment, the mixer operates on high-order of P_{LO} harmonic mixing and the suppression of I_c by P_{LO} harmonics $\frac{\partial(I_c)}{\partial(P_{LO})^{1/2}}$ is not a directly measurable parameter. However, the conversion efficiency, η, may be estimated by measuring P_{IF} peak of harmonic mixing and the corresponding THz signal power coupled into the junction using Shapiro steps on the DC IVCs.

Figure 8 shows the IVCs of the Josephson mixer at temperatures from 40 K to 77 K under the illumination of a THz signal. Clear Shapiro-steps are induced at the voltages $V_n = n\Phi_0 f_s = n \times$ (1.27 mV) (n = …, -2, -1, 0, 1, 2, ...) and the signal frequency f_s = 614.4 GHz. Note that decreasing the operating temperature results in increase of the Shapiro current-step heights (more THz power is coupled into the junction). From the current step-height, I_n, we can estimate the THz signal power coupled into the Josephson junction, $I_n/I_c = J_n(2eV_{RF}/hf)$, where J_n is an nth order Bessel function and V_{RF} is the RF voltage (that is the THz signal voltage here). This can then be used to estimate the mixer conversion efficiency $\eta = P_{IF}/P_{RF}$. In this experiment, we used a wire-grid polarizer to reduce the THz signal power in order to operate the THz mixer in smaller or weak signal range.

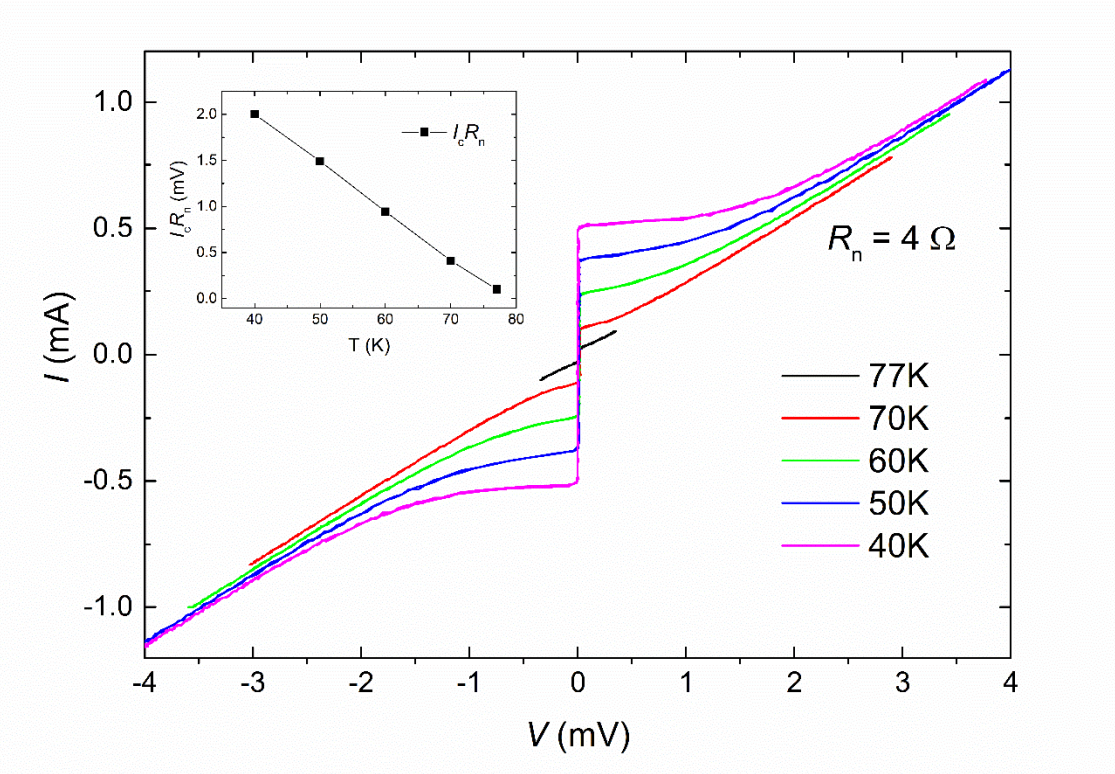

Figure 7. DC IVCs at different temperatures and the inset shows the relationship of the I_cR_n value against temperature T (K).

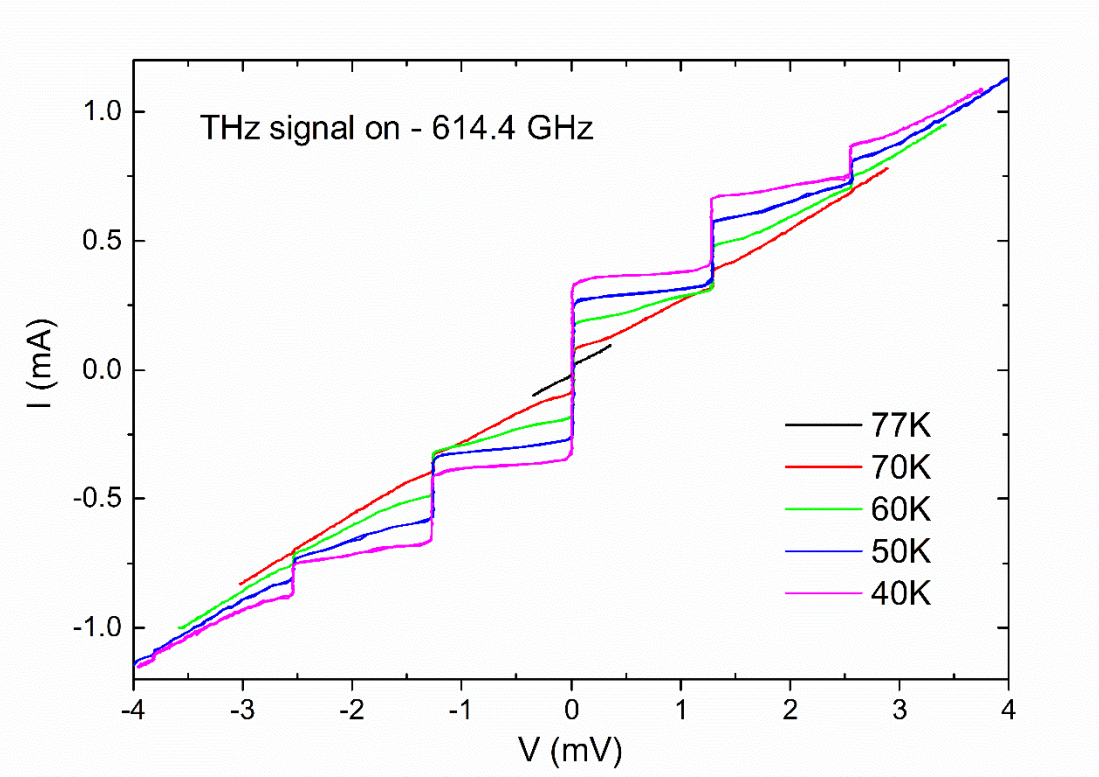

Figure. 8 DC IVCs at different temperatures under illumination of a THz signal.

Fig. 9 is the IVCs at 40K under applied THz and LO (fundamental) signal powers corresponding to the RF results presented in Figs. 10 and 11. Junction I_c is supressed by both THz signal and LO power. At fixed THz power, the level of LO power affects the IF output and operation range, as shown in the measured mixing optimal bias conditions in Fig. 12. From the 0-order Shapiro step-height induced by the THz signal shown in Fig. 9, we estimated that the THz power coupled into the mixer junction is approximately 47 nW (Note that this is much attenuated THz power using a wire-grid).

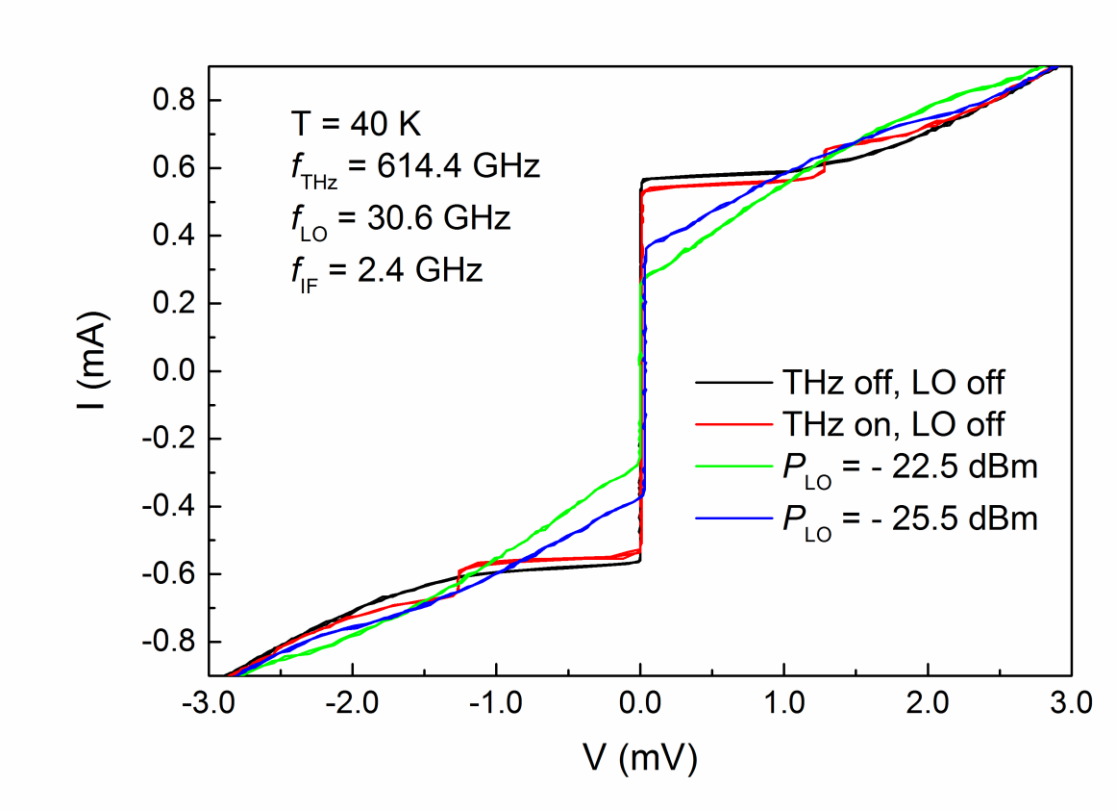

Figure 9. DC IVCs under the THz illumination and LO pumping, corresponding to the applied THz and LO (fundamental frequency) signal power for mixing results presented in figures 11 and 12.

RF Measurement Results

Mixing properties have been studied for a range of LO and THz signal conditions at temperatures ranging from 40K to 77K. For clarity, only a few selected results, mainly at T = 40K, are presented in this paper. For harmonic mixer, $f_{IF} = f_{THz} \pm nf_{LO}$ (where n is the harmonic number). We have used two different LO frequencies in this experiment to mix with a THz signal of f_{THz} = 614.4 GHz: (1) f_{LO} = 19.75 GHz, for the 31st order harmonic mixing product, f_{IF1} = 614.4 –31x19.75 = 2.15 GHz; (2) f_{LO} = 30.6 GHz, for the 20th order harmonic mixing product, f_{IF2} = 614.4 – 20x30.6 = 2.4 GHz. A higher IF output

was obtained for the 20th harmonic mixing. Figure 10 shows an example of a down-converted IF frequency spectrum at 2.4 GHz for the 20th order of harmonic mixing.

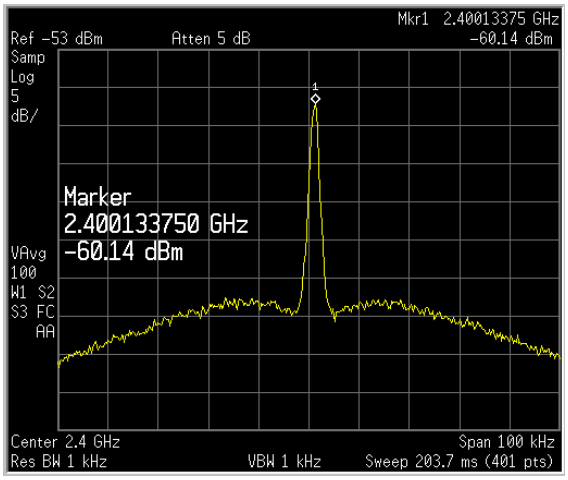

Figure 10. An IF frequency spectrum at 2.4 GHz from the 20th order harmonic mixing of a 30.6 GHz LO signal with a THz signal of 614.4 GHz.

The operating conditions in terms of the DC current bias I_B and LO power P_{LO} were studied. The IF output versus I_B and P_{LO} at T = 40K using f_{LO} = 30.6 GHz with 20th order harmonic mixing are plotted in Figures 11 and 12, respectively. Figure 11 shows the mixer IF output power P_{IF} as a function of the bias current I_B. The mixer works at a very wide range of current bias conditions and displays strong modulations whose periodicity is related to the quantized voltage between Shapiro steps induced by the f_{LO}. This will be further studied and simulated in the on-going work. Figure 11 also shows that both the IF output power and operating biasing range increase with increasing LO power. This can be qualitatively seen from the DC IVCs shown in Figure 9, where a higher LO power results in higher I_c suppression by P_{LO} and therefore a wider I_B operating range. Figure 12 shows the 20th mixing IF output against LO power (at fundamental frequency). It increases with increasing LO power and intends to plantae (or slow increase) at higher LO power. It shows a maximum peak at a LO power of - 22.5 dBm and $P_{LO} \geq$ -23 dBm is required for optimal IF output or conversion efficiency.

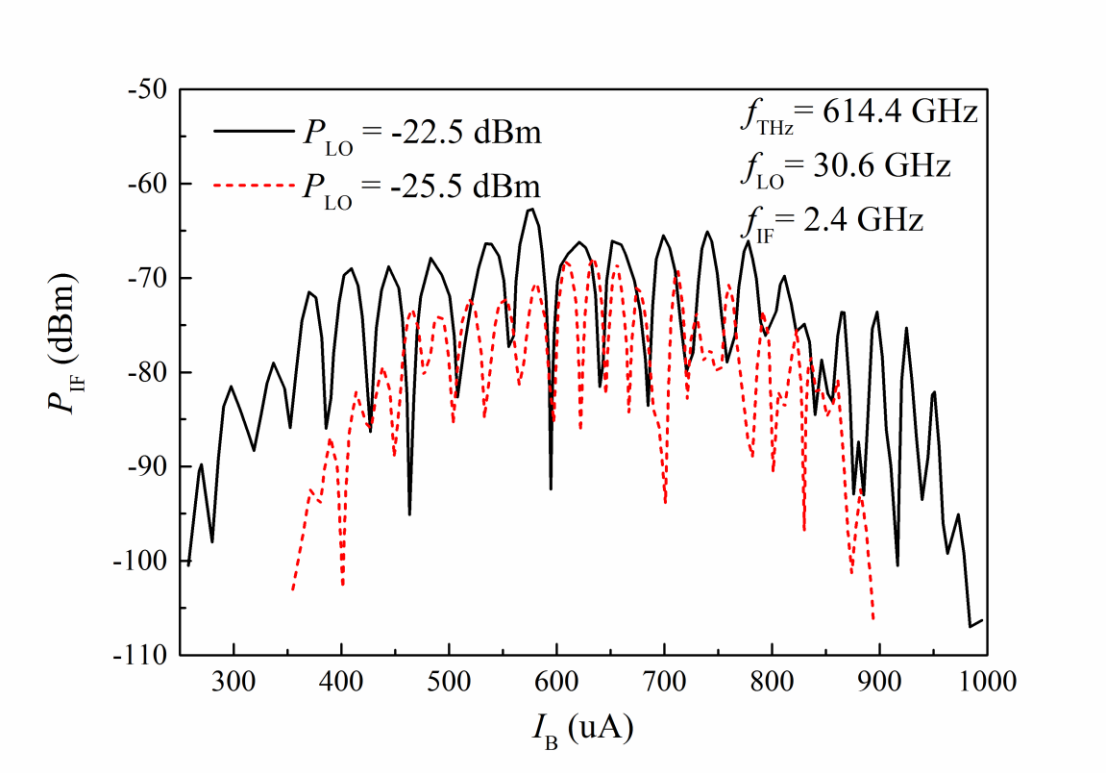

Figure 11: The 20th order harmonic mixing IF output versus the bias current at 40K for two different LO power levels.

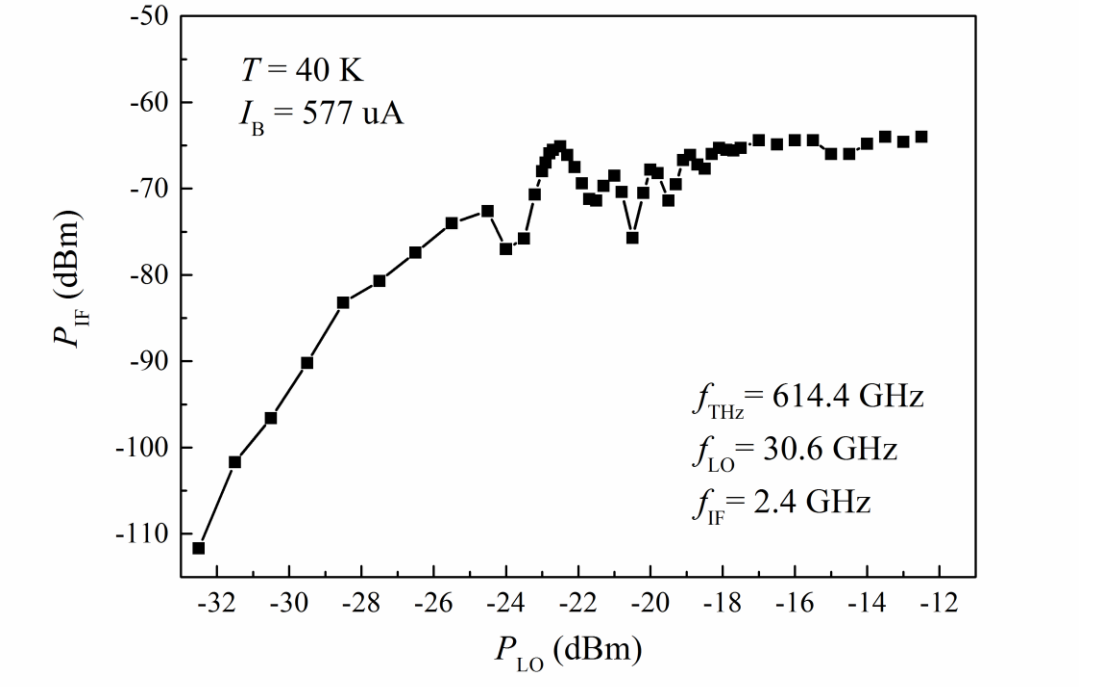

Figure 12. The 20th order harmonic mixing IF output versus LO power (at fundamental frequency) at 40K and at fixed bias current I_B.

Using the estimated THz power (47 nW) coupled into the mixer junction from Fig. 9, a conversion efficiency of approximately -49 dB is obtained for the 20th order harmonic mixing (at P_{LO} = -22.5 dBm and I_B = 577 μA). This value includes the junction IF output coupling loss and the loss of IF matching circuit chain (between ports P1 and P1 in Figure 2). This value is close to that of the state-of-art semiconductor Schottky diode harmonic mixers developed by Virginia Diode, Inc. (~ - 45 dB at 500 GHz) [18] (no date available for > 600 GHz high-order harmonic mixer). Further study of the mixer conversion efficiency versus different harmonic numbers is currently underway.

The presented mixer demonstrated stable operation at temperatures up to 77K, even for 31st order harmonic mixing. Figure 13 shows IF output spectra for the mixer operating at 60, 70 and 77K. The IF output or conversion gain increases with decreasing temperature due to increasing dynamic resistance and junction characteristic voltage or frequency. Nevertheless, the mixer was able to operate at 77K reliably, indicating the potential of operating the HTS THz mixer in liquid nitrogen or a miniature single-stage cryocooler. In contrast, many reported HTS Josephson millimeter or THz mixers including those based on fundamental LO frequency mixing operated at temperatures well below 77K. This result shows the excellent quality of our step-edge junction coupled with a well-designed antenna and matching/isolation circuit, which maximizes the mixer conversion efficiency.

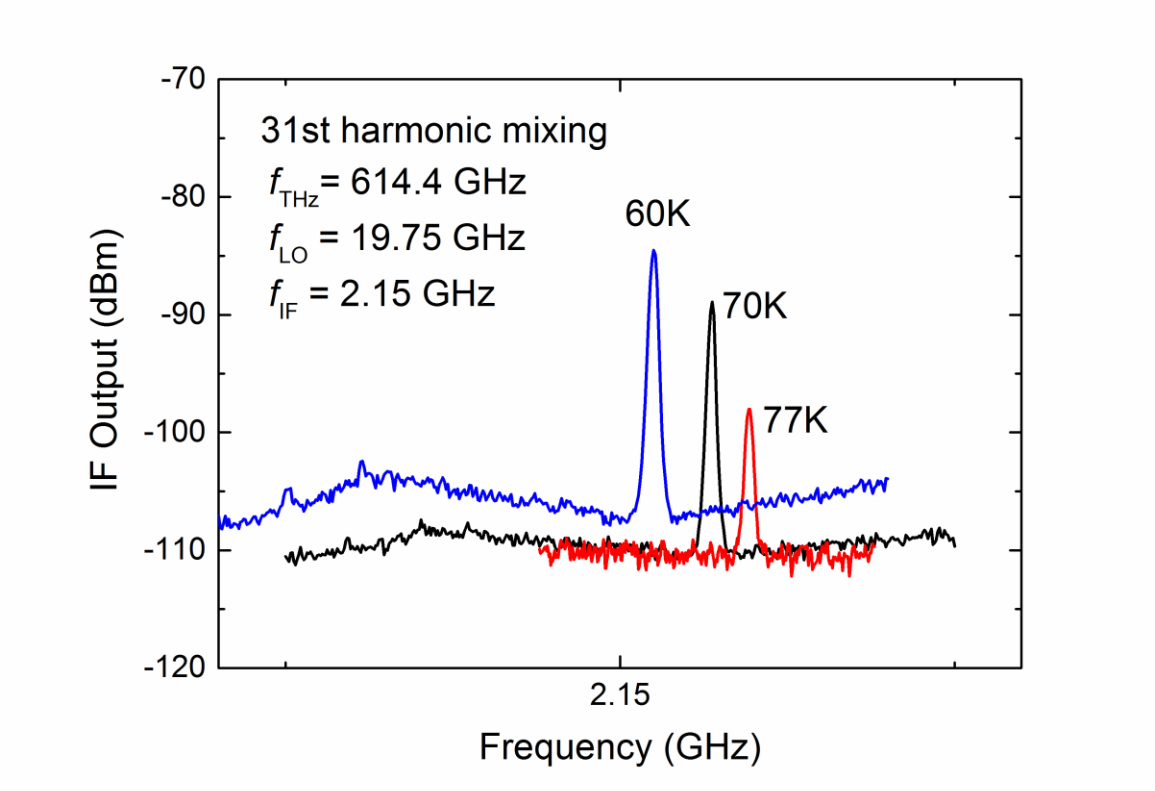

Figure 13. The 31th harmonic mixing IF output spectrum at 60, 70 and 77K. Note that the peaks are intentionally shifted slightly on the x-axis (frequency) for clarity.

The linearity of the harmonic mixer was also measured at low THz power range and the result is shown in Figure 14. Note that this measurement was carried out on a different step-edge junction mixer which has a lower I_c value so a lower P_{LO} is required for optimal biasing. The THz power was largely attenuated from the maximum signal level by using a wire grid (and cardboard attenuators. A linear relationship is displayed at lower signal power range.

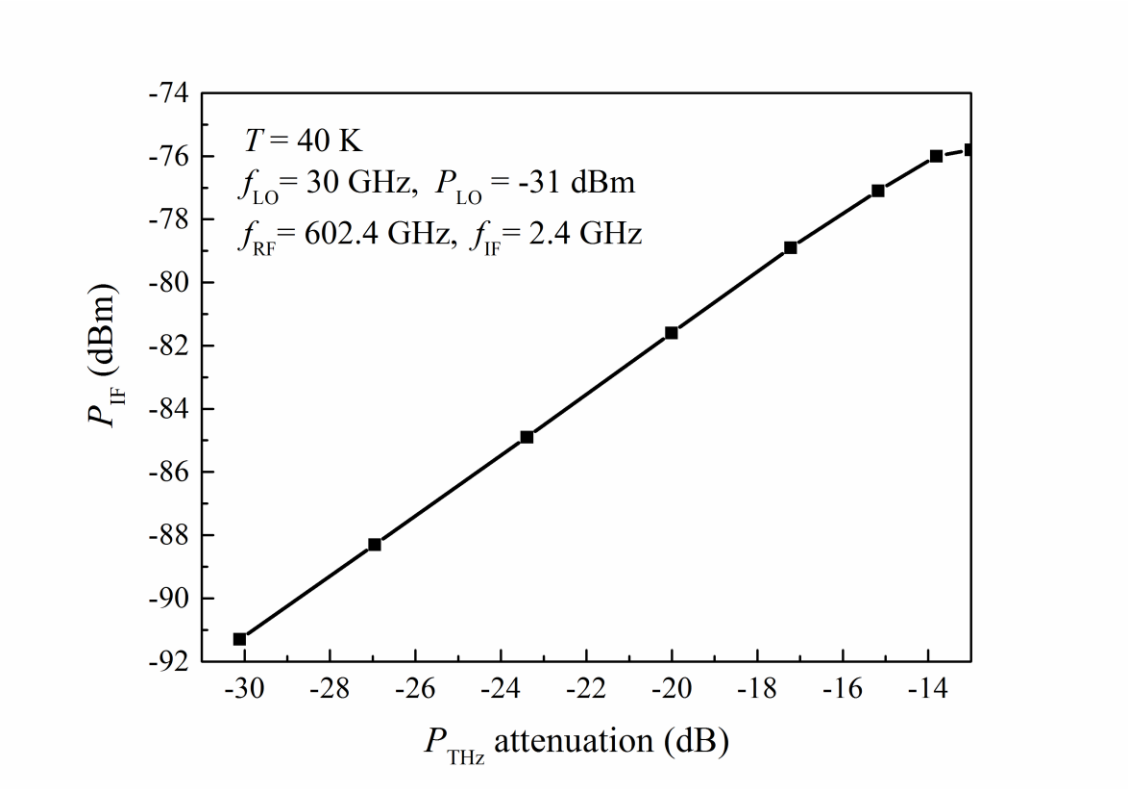

Figure 14. IF output versus the input THz power change (attenuated using different wire grid angle plus another power attenuator).

Conclusion

A thin-film antenna coupled YBCO step-edge Josephson junction heterodyne THz mixer was designed and experimentally demonstrated. The frequency down-conversion from 600 GHz to ~ 2 GHz was obtained using high-order (up to 31st) harmonic mixing. The measured junction parameters showed excellent characteristics with its characteristic frequency reaches ~ 1 THz at 40 K, thus suitable for THz frequency down-conversion. The mixer works under a wide range of bias current and LO power conditions and displays a linearity of the IF output power versus the THz signal power at low signal power range. The desirable junction characteristics coupled with a well-designed antenna and matching/isolation circuit enable successful operation of the mixer at relatively high temperatures

(up to 77K) and maximize the conversion efficiency. The results demonstrated the potential of the HTS Josephson mixer for THz detection and THz communication receivers.

Acknowledgement

We thank Dr Stephen Hanham of Imperial College (U.K.) for advice on antenna design, Ms Jeina Lazar (CSIRO) for HTS chip fabrication and Ms Mei Shen (CSIRO) for packaging the module.

References

1. Kleine-Ostmann T and Nagatsuma T 2011 A Review on Terahertz Communications Research, *J Infrared Milli Terahz Waves* **32** 143–171.

2. Chen J, Kurigata Y, Wang H B, Nakajima K, Yamashita T, and Wu P H 2003 Wideband frequency metrology using high temperature superconducting Josephson junctions, *IEEE Trans. Appl. Supercond.* **13,** 1143-1146.

3. Divin Y Y, Poppe U, Volkov O Y, and Pavlovskii V V 2000 Frequency-selective incoherent detection of terahertz radiation by high-Tc Josephson junctions *Appl. Phys. Lett*. **76**, 2826-2828.

4. Du J, Smart K, Li L, Leslie K E, Wang D, Foley C P, Ji F, Li X D and Zeng D Z 2015 A cryogen-free HTS Josephson junction detector for terahertz imaging, *Supercond. Sci. Technol.* **28** 084001.

5. Du J, Hellicar A D, Li L, Hanham S, Macfarlane J C, Leslie K E, Nikolic N, Foley C P, and Greene K J 2009 Terahertz imaging at 77 K *Supercond. Sci. Technol.* **22** 114001.

6. Zhang T, Du J, Wang J, Bai D D, Guo Y J and He Y S 2015 30 GHz HTS Receiver Front-end based on Monolithic Josephson Mixer *IEEE Trans Appl. Supercond*. **25** 1400605.

7. Du J**,** Zhang T, Guo Y J and Sun X W 2013 A high-temperature superconducting monolithic microwave integrated Josephson down-converter with high conversion efficiency, *Appl. Phys. Lett.* **102** 212602.

8. Harnack O, Darula M, Scherbel J, Heinsohn J K, Siegel M, Diehl D and Zimmermann P 1999 Optimization of a 115 GHz waveguide mixer based on an HTS Josephson junction *Supercond. Sci. Technol.* **12** 847-849.

9. Scherbel J, Darula M, Harnack O and Siegel M 2002 Noise properties of HTS Josephson mixers at 345 GHz and operating temperatures at 20 K *IEEE Trans. Appl. Supercon.* **12** 1828-1831.

10. Malnou M, Feuillet-Palma C, Ulysse C, Faini G, Febvre P, Sorena M, Olanier L, Lesueur J and Bergeal N 2014 High-Tc superconducting Josephson mixers for terahertz heterodyne detection *J. Appl. Phys.* **116** 074505.

11. Taur Y, Claassen J H and Richards P L 1974 Conversion gain and noise in a Josephson mixer *Rev. Phys. Appl*. **9** 263.

12. Kita S and Fujisawa K 1982 Performance of Josephson junction harmonic mixers with harmonic number 1-8 at 70GHz *Jap. J. Appl Phys*. **21** 497-503.

13. Chen J, Kobayashi E, Nakajima K, Yamashita T, Linzen S, Schmidl F and Seidel P 1999 Terahertz responses of HTS Josephson junctions on bicrystal substrates *Advances in Superconductivity XI,* eds. N. Koshizuka et al*,* Springer Japan, 1999, pp.1279-1284.

14. Foley C P, Mitchell E E, Lam S K H, Sankrithyan B, Wilson Y M, Tilbrook D L, and Morris S J 1999 Fabrication and characterisation of YBCO single grain boundary step edge junctions *IEEE Trans. Appl. Supercond.* **9** 4281-4284.

15. Mitchell E E and Foley C P 2010 YBCO Step-edge junctions with high IcRn *Supercond. Sci. Technol* **23** 065007.

16. Du J, Lam S K H, and Tilbrook D L 2001 Metallization and interconnection of HTS YBCO thin film devices and circuits, *Supercon. Sci. & Technol* **14** 820-825.

17. Van Duzer T and Turner C W 1999 *Superconductive Devices and Circuits,* Prentice-Hall, Inc.

18. "Even Harmonic Mixers", Virginia Diodes, Inc. http://www.vadiodes.com/en/products/mixers